ORIGINAL RESEARCH

Irisin Inhibits Atherosclerosis by Promoting Endothelial Proliferation Through microRNA126-5p

Yuzhu Zhang, MD; Haibo Song, MD, PhD; Yuan Zhang, MD; Fei Wu, MD; Qian Mu, MD; Miao Jiang, MD; Fang Wang, MD; Wen Zhang, MD, PhD; Liang Li, MD; Lei Shao, MD; Shiwu Li, MD, PhD; Lijun Yang, MD, PhD; Mingxiang Zhang, MD, PhD; Qi Wu, MD, PhD; Dongqi Tang, MD, PhD

***Background*—**Irisin is a newly discovered myokine that has been considered a promising candidate for the treatment of cardiovascular disease through improving endothelial function. However, little is known about the role of irisin in the progression of atherosclerosis.

***Methods and Results*—**We used a carotid partial ligation model of apolipoprotein E–deficient mice fed on a high-cholesterol diet to test the anti-atherosclerosis effect of irisin. Irisin treatment significantly suppressed carotid neointima formation. It was associated with increased endothelial cell proliferation. In addition, irisin promoted human umbilical vein endothelial cell survival via upregulating microRNA126-5p expression through the ERK signaling pathway. Inhibition of microRNA126-5p using the microRNA126-5p inhibitor abolished the prosurvival effect. The same results were demonstrated in vivo as the expression of microRNA126-5p noticeably increased in ligated carotid artery after irisin treatment. Furthermore, in vivo blockade of microRNA126-5p expression using the antagomir abolished the inhibitory effects of irisin on neointima formation, lesional lipid deposition, macrophage area, and the pro-proliferation effects on endothelial cells.

***Conclusions*—**Taken together, our study demonstrates that irisin significantly reduces atherosclerosis in apolipoprotein E–deficient mice via promoting endothelial cell proliferation through microRNA126-5p, which may have a direct therapeutic effect on atherosclerotic diseases. **(*J Am Heart Assoc*. 2016;5:e004031 doi: 10.1161/JAHA.116.004031)**

Key Words: atherosclerosis • endothelial cells • irisin • microRNA126-5p

Atherosclerosis, the primary cause of cardiovascular diseases, remains a leading cause of morbidity and mortality worldwide.[1–3] Endothelial cells (ECs) function as a selectively permeable barrier between circulating blood and surrounding tissues, therefore their integrity is critical for the maintenance of blood vessel homeostasis.[1,4] Endothelial dysfunction has been implicated as an early step in the pathogenesis of atherosclerosis.[5]

Endothelial integrity can be maintained through replacement of damaged ECs with proliferating, healthy ECs.[6] Therefore, improving endothelial function is critical for the prevention and treatment of atherosclerosis. Irisin, a newly discovered myokine, is mainly secreted by skeletal muscle as a cleavage product of fibronectin type III domain-containing protein 5.[7] Irisin activates profound changes in the subcutaneous adipose tissue, stimulating browning and uncoupling protein 1 expression.[8,9] The presence of human irisin in blood was demonstrated by a recent study using quantitative mass spectrometry.[10] It has been reported that serum irisin levels are significantly lower in patients with obesity, insulin resistance, type 2 diabetes mellitus, and metabolic syndrome.[8,11–13] Intriguingly, a growing number of studies have shown that irisin improves endothelial function in patients with type 2 diabetes and obese patients.[14–18] In addition, we have demonstrated that irisin can promote human umbilical vein endothelial cell (HUVEC) proliferation and angiogenesis via the ERK signaling pathway.[19,20] However, whether irisin can effectively promote endothelial proliferation in

From the Center for Gene Therapy and Immunotherapy, The Second Hospital of Shandong University, Jinan, China (Yuzhu Z., H.S., Yuan Z., F. Wu, Q.M., M.J., F. Wang, W.Z., L.L., L.S., D.T.); Department of Pathology, Immunology, and Laboratory Medicine, University of Florida College of Medicine, Gainesville, FL (S.L., L.Y.); The Key Laboratory of Cardiovascular Remodeling and Function Research, Chinese Ministry of Education and Chinese Ministry of Health, Qilu Hospital of Shandong University, Jinan, China (M.Z.); Department of Anatomy, School of Medicine Shandong University, Jinan, China (Q.W.).

Accompanying Figures S1 and S2 are available at http://jaha.ahajournals.org/content/5/9/e004031/DC1/embed/inline-supplementary-material-1.pdf

Correspondence to: Dongqi Tang, MD, PhD, Center for Gene Therapy and Immunotherapy, The Second Hospital of Shandong University, 247 Beiyuan Street, Jinan 250012, China. E-mail: tangdq@sdu.edu.cn

Received June 6, 2016; accepted September 1, 2016.

atherosclerosis, and its underlying mechanisms, remains unknown. MicroRNA (miRNA)s are endogenous, single-stranded, small noncoding RNA molecules of ≈19 to 22 nucleotides.[21] Recent studies have reported that miRNAs can regulate the expression of molecules involved in vascular inflammation, tone, and remodeling, thus inducing endothelial dysfunction.[22,23] miRNAs can also mediate proliferation, migration, angiogenesis, and senescence of ECs.[16,24–27] These studies suggest that miRNAs may be involved in atherogenesis by modulating endothelial functions.

In the present study, we explored the effect of irisin on endothelial proliferation and atherosclerosis formation in the mouse carotid partial ligation model. In vitro, we investigated the expression profiles of miRNAs, which may participate in irisin-induced EC proliferation. Our results demonstrated that irisin can prevent the formation of atherosclerosis by promoting endothelial proliferation through microRNA126-5p (miR126-5p).

Methods

Expression and Purification of Human Irisin

The expression and purification of irisin were performed as previously described.[9,28] Briefly, human irisin cDNA (360 bp) was designed, synthesized (Life Technologies), and cloned into the EcoR1/Xba1 sites of the pPICZαA plasmid. The linearized pPICZaA-irisin plasmid was transformed into Pichia pastoris X-33 according to the manufacturer's instructions (PichiaEasycomp Transformation Kit; Invitrogen). Yeast culture was used for the production of human irisin protein as previously described.[9] The r-irisin protein in the culture supernatant was purified and used in this study.

Mouse Model

Male apolipoprotein E (apoE)–deficient mice (6–8 weeks old) purchased from Vital River Laboratory Animal Technology Co., Ltd (China) were fed a high-cholesterol diet containing 21% fat and 0.15% cholesterol. For the neointima study, male apoE-deficient mice (6–8 weeks old) were anesthetized by intraperitoneal (IP) injection of pentobarbital sodium (50 mg/kg, Nembutal sodium solution; Wuhan Entai Technology, Wuhan, China). Partial ligation of the left common carotid artery was carried out as previously described.[29] Briefly, a ventral midline incision (4–5 mm) was made in the neck. The left carotid artery was exposed by blunt dissection. Three of four caudal branches of the left carotid artery, the left external artery, internal carotid artery, and occipital artery were ligated with a 6–0 silk suture, while the superior thyroid artery was left intact. Twenty-four hours after partial ligation, the mice were treated daily with purified irisin (0.5 μg/g body weight) by IP injection for 4 weeks. In the control group, the partial ligated mice were given normal saline (NS) in the same manner. After the treatment, mice were anesthetized with pentobarbital sodium and the segment of the left carotid artery just proximal to the ligation was excised. All animal experiments were carried out in accordance with the National Institutes of Health Guide for the Care and Use of Laboratory Animals and were approved by the Shandong University of Laboratory Animals Care and Use Committee.

miR126-5p Antagomir Treatment

Fifty μL F-127 pluronic gel (20%, p2443, Sigma) containing 0.1 mg antagomir against miR126-5p (miR126-5p antagomir, RiboBio, Guangzhou, China) or control (miR126-5p antagomir control, RiboBio) was applied to the adventitia around ligated artery segments.

Histological Examination

The harvested carotid arteries were fixed in 4% paraformaldehyde and then embedded in paraffin. Five cross sections (5-μm thickness) per block were cut at 100-μm intervals and stained with hematoxylin-eosin. Images were captured using a Nikon eclipse Ti microscope and analyzed using Image Pro Plus software (version 6.0; Media Cybernetics). The neointima area was defined as the area between the luminal surface and internal elastic lamina. The medial area was defined by the internal elastic lamina and external elastic lamina. The N/M ratio was expressed as the ratio of the neointima area to media area.

Immunostaining

Immunohistofluorescence was performed using primary antibodies for CD31 (1:100, ab24590, Abcam), Ki67 (1:200, ab15580, Abcam), and α-smooth muscle actin (α-SMA, 1:100, A5228, sigma) on paraffin-embedded sections. Fluorescently labeled secondary antibodies (Invitrogen) were used for visualization. Immunohistochemical staining was performed using GTVisionTM III Detection System/Mo&Rb (GK500705, Gene Tech). Paraffin-embedded sections were stained with primary antibodies for CD68 (1:200, ab955, Sigma). After washing, sections were incubated with horseradish peroxidase–conjugated secondary antibodies. Immunocomplexes were then detected using diaminobenzidine tetrahydrochloride dehydrate substrate. For quantification of lipid content, serial frozen sections (10-μm thickness) were first stained with Oil Red O and then counterstained with hematoxylin. Images were captured using a Nikon Eclipse Ti fluorescent microscope, and the stained area was measured using Image Pro Plus software.

TUNEL Staining

Apoptotic cells in partial ligated carotid arteries were detected by terminal deoxynucleotidyl transferase–mediated dUTP nick end labeling (TUNEL) using a kit (R&D Systems) as previously described according to the manufacturer's instructions.[28] After TUNEL labeling, sections were counterstained with 4′-6-diamidino-2-phenylindole (DAPI) to detect nuclei.

Cell Culture

The primary culture of HUVECs was performed as previously described.[19] Briefly, HUVECs were isolated from human umbilical cord using 300 units/mL collagenase II (Sigma-Aldrich). Cells were cultured in Medium 199 (Invitrogen) that was supplemented with 10% (v/v) fetal bovine serum (Invitrogen), 10 ng/mL EGF (Peprotech), and 10 ng/mL bFGF (Peprotech) in a humidified atmosphere of 5% CO_2 at 37°C. Passages between 3 and 7 were used in this study. All experiments were carried out with the same batch of HUVECs, which were from a single donor.

The study protocol conformed to the ethical guidelines of the 1975 Declaration of Helsinki with the approval of the Institutional Medical Ethics Committee of Qilu Hospital, Shandong University. The donor has provided written informed consent.

Quantitative Real-Time PCR

To detect mRNA expression levels, total RNA was extracted using TRIzol reagent (Invitrogen) following the standard protocol, and the cDNA was synthesized using the SuperScript III First-Strand Synthesis System (Invitrogen Corp., Carlsbad, CA). Quantitative real-time polymerase chain reaction (qRT-PCR) was carried out in triplicate with SYBR Green Master Mix (Applied Biosystems) using the Bio-Rad CFX96 Real-Time System (Bio-Rad, Hercules, CA). The $2^{-\Delta\Delta Ct}$ method was used to calculate the relative expression of genes using beta-actin RNA as an internal control. The primers for delta-like 1 homolog (*Dlk1*) are 5′-TCGGCCACAGCACCTATGG-3′ (forward) and 5′-CAGCCGTCGGTGCAAATGC-3′ (reverse); for *MMP7* are 5′-ATGTGGAGTGCCAGATGTTGC-3′ (forward) and 5′-AGCAGTTCC CCATACAACTTTC-3′ (reverse); for *ADAM9* are 5′-CCCCCAAA TTGTGAGACTAAAG-3′ (forward) and 5′-TCCGTCCCTCAATG CAGTAT-3′ (reverse); for stromal-derived factor-1 α (*SDF-1α*) are 5′-AGAATTCATGAACGCCAAGG-3′ (forward) and 5′-AGGATCCTCACATCTTGAACC-3′ (reverse); and for *β-actin* are 5′-ATCATGTTTGAGACCTTCAACA-3′ (forward) and 5′-CAT CTCTTGCTCGAAGTCCA-3′ (reverse).

miRNA Microarray Analysis

HUVEC miRNA expression was assessed following stimulation for 12 hours with or without 20 nmol/L irisin using Exiqon miRCURY LNA arrays. Briefly, total RNA was harvested using TRIzol (Invitrogen) and the miRNeasy Mini Kit (QIAGEN) according to the manufacturer's instructions. After RNA quantity measurement using the NanoDrop 1000 (Thermo Fisher Scientific), the samples were labeled using the miRCURY Hy3/Hy5 Power labeling kit (Exiqon) and hybridized on the miRCURY LNA array (Exiqon, version 18.0). The slides were scanned using the Axon GenePix 4000B microarray scanner. Scanned images were then imported into GenePix Pro 6.0 software (Axon) for grid alignment and data extraction. Finally, hierarchical clustering was performed to show distinguishable miRNA expression profiling among samples. Array results were validated by qRT-PCR.

miRNA qRT-PCR

miRNAs were prepared with an All-in-One TM miRNA qRT-PCR Detection Kit (GeneCopoeia) according to the manufacturer's instructions. Briefly, total RNA was extracted using TRIzol (Invitrogen) following the standard protocol and the extracted RNA was reverse-transcribed in the presence of poly(A) polymerase with an oligo(dT) adaptor. Then qRT-PCR was carried out with SYBR green detection with a forward primer for the mature micoRNA sequence and a universal adaptor reverse primer. RNU6 was used as an endogenous control. miRNA primers and the RNU6 primer were purchased from GeneCopoeia.

miRNA Inhibitor and siRNA Transfection

The miR126-5p inhibitor and its negative control, and the Dlk1 silencing RNA (siRNA) and its negative control were obtained from RiboBio (Guangzhou, China). Transfection was conducted using Lipofectamine 2000 (Invitrogen) according to the manufacturer's instructions. The final concentration of miR126-5p inhibitor and Dlk1 siRNA were 100 nmol/L. Cells were incubated with transfection complexes for 4 to 6 hours before the medium was changed.

BrdU Incorporation Assay

HUVECs grown on coverslips were incubated with BrdU (10 μmol/mL, B5002, Sigma-Aldrich, St. Louis, MO) and irisin or PBS for 24 hours before fixation in 4% paraformaldehyde and permeabilized with 0.5% Triton X-100. After permeabilization, cells were denatured with 2 mol/L HCl for 60 minutes at room temperature followed by neutralization with 0.1 mol/L sodium borate (pH 8.5) for 10 minutes. After washing and blocking with goat serum, cells were incubated with rabbit anti-Brdu (1:500, ab152095, Abcam) antibodies overnight at 4°C. Cells were visualized with Alexa Fluor 488 conjugated goat anti-rabbit IgG (Invitrogen) for 1 hour at room

temperature. Finally, the cells were photographed using a confocal microscope and images were analyzed using Volocity software (PerkinElmer). Total cells were quantified by counterstaining with blue fluorescent DAPI.

CCK-8 Assay

HUVECs were seeded in 96-well plates with 5000 cells/well. Cell proliferation was assayed using the Cell Counting Kit-8 (CCK-8; Dojindo Molecular Technologies, Gaithersburg, MD) according to the manufacturer's protocol. Briefly, the CCK-8 solution was added to the culture medium after stimulation, and the cultures were then incubated for 2 hours at 37°C in humidified 95% air and 5% CO_2. The absorbance at 450 nm was determined using a Microplate Reader (Bio-Rad, Hercules, CA). For each group, 6 duplicate wells were detected per experiment.

Western Blot

HUVECs were lysed in RIPA buffer (150 mmol/L NaCl, 50 mmol/L Tris (pH 8.0), 150 mmol/L NaCl, 1% NP-40, 0.5% sodium deoxycholate, 0.1% SDS) containing 1 mmol/L Na_3VO_4, 5 mmol/L NaF, and protease inhibitor cocktail (Roche). The supernatant was removed and the protein concentration was determined using the BCA protein assay kit (Pierce, Rockford, IL). Equal amount of proteins from cell lysates were separated using 12% SDS-PAGE gels. After electrophoresis, proteins were transferred onto PVDF membranes. After blocking with 5% fat-free milk for 1 hour, proteins were detected using the appropriate primary antibodies, respectively, against Dlk1 (1:1000, ab21682, Abcam), ERK1/2 (1:1000, 4695S, Cell Signaling), phospho-ERK1/2 (Thr202/Tyr204) (1:1000, 9101S, Cell Signaling), eNOS (1:1000, 9572, Cell Signaling), phospho-eNOS (Ser1177) (1:1000, 9571, Cell Signaling), or GAPDH (1:1000, sc-25778, Santa Cruz). After incubation with a horseradish peroxidase–conjugated secondary antibody (1:5000, Santa Cruz) at room temperature for 1 hour, the immune complexes were detected using the ECL method. Densitometric analysis was performed using Alpha Imager 2200.

Apoptosis Analysis

Apoptotic cells were determined by using an Annexin V-FITC apoptosis detection kit (BD Biosciences-US) according to the manufacturer's instructions as previously described.[28] Briefly, HUVECs were seeded into 6-well plates and incubated with or without 20 nmol/L irisin, 100 nmol/L miR126-5p inhibitor, and 80 μg/mL oxidized low-density lipoprotein (ox-LDL; Yiyuan Biotechnologies, Guangzhou, China) for 24 hours. After incubation, cells were washed twice with cold PBS and then resuspended. Subsequently, cells were incubated for 15 minutes at room temperature in the dark in 100 μL binding buffer containing 5 μL Annexin V-FITC and 5 μL PI. Cellular fluorescence was analyzed by the BD accuriC6 flow cytometer using FlowJo software.

Statistical Analysis

All experiments were performed at least three times. Data are expressed as mean±SEM. Statistical comparisons were made between two groups using Student *t* test and between multiple groups by ANOVA followed by Student-Newman-Keuls post hoc test. *P* values <0.05 were considered statistically significant. The Shapiro-Wilk test was used to determine whether the data met criteria for normal distribution. Data with a Shapiro-Wilk test *P* value >0.05 was considered to fit a normal distribution.

Results

Irisin Inhibits Neointima Formation in apoE-Deficient Mice After Carotid Artery Partial Ligation

Irisin significantly reduced the neointima formation in apoE-deficient mice after carotid artery partial ligation for 4 weeks (1.91 ± 0.17 $\mu m^2\times10^4$ in irisin-treated mice versus 3.93 ± 0.28 $\mu m^2\times10^4$ in NS-treated mice) (Figure 1A and 1B). The ratio of neointima to media was also decreased in the irisin treatment group (1.04 ± 0.16) compared with the NS group (2.03 ± 0.21) (Figure 1C). To determine the contribution of irisin to EC proliferation, we detected the Ki67-positive ECs in partially ligated carotid artery samples. We found that irisin significantly increased EC proliferation in luminal ECs of partially ligated carotid arteries ($7.96\pm1.28\%$ in irisin-treated mice versus $3.07\pm0.45\%$ in NS-treated mice) (Figure 1D). These results suggested that irisin probably inhibits neointima formation by promoting EC proliferation.

Irisin Promotes HUVEC Proliferation

We tested the role of irisin on HUVEC proliferation by using the BrdU incorporation assay. The results showed that the proportion of BrdU-positive cells in the irisin-treated (20 nmol/L) group ($69.30\pm2.54\%$) was significantly higher than in the control group ($42.02\pm2.35\%$) (Figure 2A and 2B). Then we used the CCK-8 assay to evaluate cell viability. Following irisin treatment for 24 hours, the HUVEC viability was 1.26-fold ($126.7\pm4.1\%$) higher than in the control group (Figure 2C), demonstrating that irisin can effectively promote HUVEC proliferation.

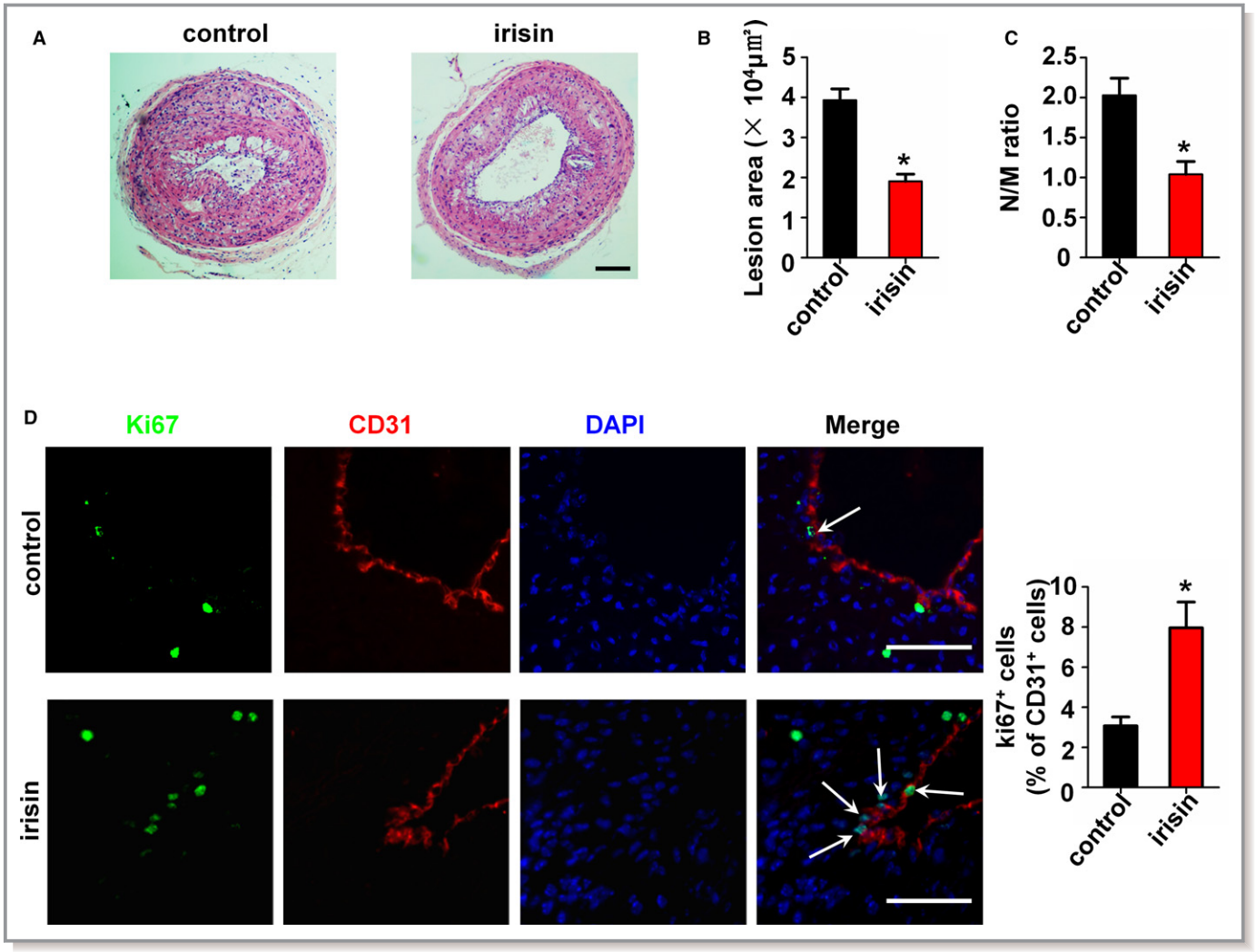

Figure 1. Influence of irisin treatment on neointima formation and endothelial cells (EC) proliferation in apolipoprotein E (ApoE)–deficient mice. ApoE–deficient mice were treated with or without irisin for 28 days after carotid artery partial ligation (n=5). (A) Cross-sections of carotid arteries were identified with hematoxylin-eosin staining. Scale bar indicates 100 μm. (B) Quantification of the neointima areas of the partially ligated carotid arteries is shown. (C) Degree of neointima formation 28 days after carotid ligation was calculated according to the neointima area to media area (N/M) ratio. (D) EC proliferation after partial ligation of the carotid artery was assessed by double immunofluorescence staining for Ki67 and CD31. Representative images of Ki67 staining show proliferating cells (stained in green) in the endothelium. The nuclei were stained blue with 4′-6-diamidino-2-phenylindole (DAPI). CD31 (stained in red) was used as an endothelial marker. Arrows indicate $Ki67^{+}CD31^{+}$ cells. Scale bar indicates 50 μm. The data are expressed as mean±SEM. *P<0.05 vs control.

miR126-5p Expression Was Upregulated by Irisin Treatment in ECs

To further investigate the mechanism by which irisin promotes HUVEC proliferation, the miRNA expression profile of HUVECs was assessed following stimulation with 20 nmol/L irisin for 12 hours using Exiqon miRCURY LNA arrays. One hundred fourteen miRNAs were upregulated ≥2-fold and 84 miRNAs were markedly downregulated in irisin-treated HUVECs. Partial results of the miRNA array are shown in Figure 3A. Among the affected miRNAs, we selected 8 miRNAs that were reported to play roles in endothelial function for further investigation. To confirm the findings of the miRNA profile, the expression of these 8 upregulated miRNAs was measured using qRT-PCR. In agreement with the microarray data, 6 upregulated miRNAs were validated (Figure 3B). miR126-5p is of particular interest among all the validated miRNAs because it had the highest expression level in irisin-treated HUVECs compared with the controls. To further validate the elevation of miR126-5p in the irisin-treated HUVECs, time-dependent changes in miR126-5p levels from HUVECs after treatment with 20 nmol/L irisin for 2, 6, 12, and 24 hours were determined. The results showed that miR126-5p expression was significantly upregulated in HUVECs after treatment with irisin for 12 and 24 hours and had peak expression at 12 hours (Figure 3C). The results indicate that irisin can increase the expression of miR126-5p in vitro.

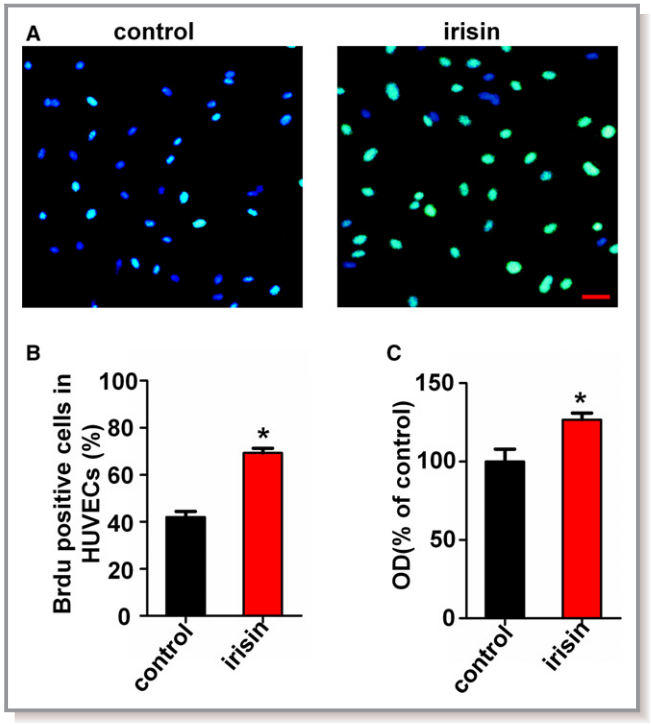

Figure 2. Irisin promotes human umbilical vein endothelial cell (HUVEC) proliferation in vitro. (A) Effect of irisin on HUVEC proliferation was measured by using the BrdU incorporation assay. Scale bar indicates 80 μm. (B) Proliferation was assessed by the ratio of the average number of BrdU-positive cells to total cells in 10 random high-magnification fields. (C) Vitality of HUVECs was measured using the CCK8 assay. The data are expressed as the mean±SE of three independent experiments. **P*<0.05 vs control.

Irisin-Mediated Promotion of Endothelial Proliferation Was Abolished by Inhibition of miR126-5p

To further explore the role of miR126-5p in irisin-induced HUVEC proliferation, the miR126-5p inhibitor was added to the cultured HUVECs. qRT-PCR showed the successful inhibition of cellular miR126-5p by the miR126-5p inhibitor as compared with the negative control (Figure S1A). Using the BrdU incorporation assay, it was demonstrated that inhibition of miR126-5p reduced HUVEC proliferation activity following irisin treatment (Figure 4A and 4B). Similar results were also obtained using the CCK-8 assay (Figure 4C). These results suggest that miR126-5p mediates the effects of irisin on HUVEC proliferation.

Activation of Phospho-ERK Mediates Irisin-Induced miR126-5p Expression

We have demonstrated that ERK phosphorylation was involved in irisin-induced HUVEC proliferation.[19] Next, ERK inhibitor U0126 and the miR126-5p inhibitor were used to confirm the association between ERK phosphorylation and miR126-5p induction after irisin treatment. As shown in Figure 5A, phosphorylated ERK was significantly increased

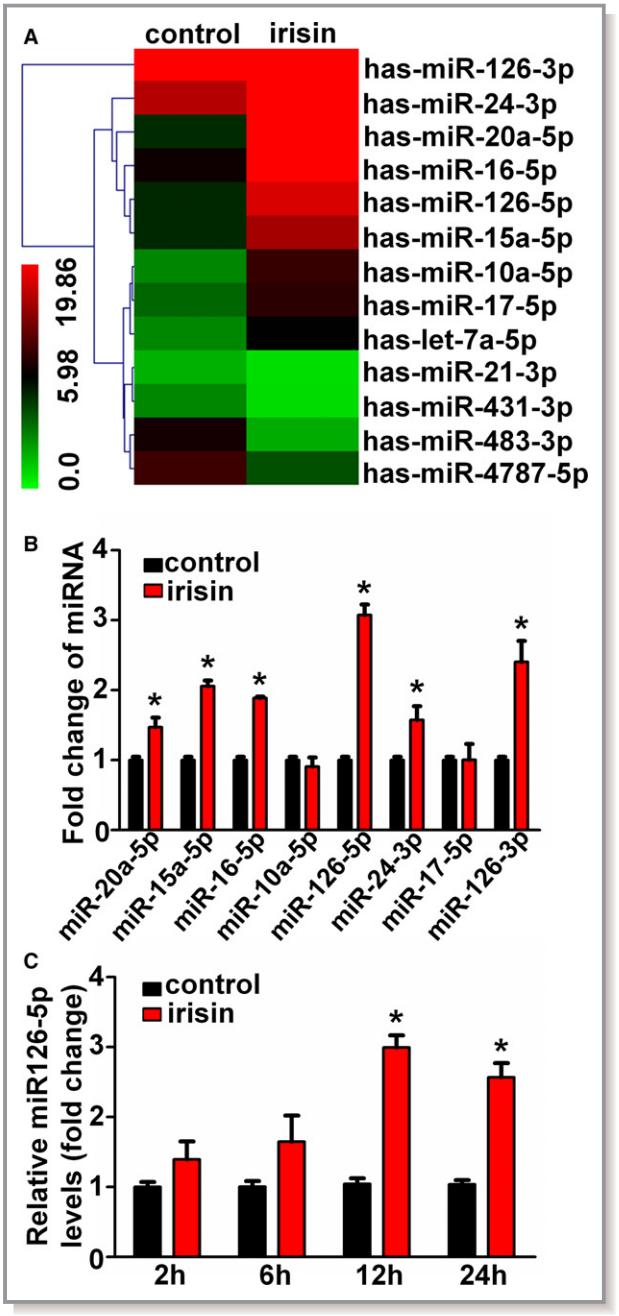

Figure 3. Irisin upregulated the microRNA126-5p (miR126-5p) expression in human umbilical vein endothelial cells (HUVECs). (A) Heat map presentation of the expression profile of microRNAs in irisin-treated and control HUVECs. "Red" indicates high relative expression, and "green" indicates low relative expression. (B) Microarray results were validated by quantitative real-time polymerase chain reaction (qRT-PCR) in HUVECs. (C) Time-dependent effects of irisin on relative miR126-5p expression were tested using qRT-PCR. The data are expressed as the mean±SEM of three independent experiments. **P*<0.05 vs control.

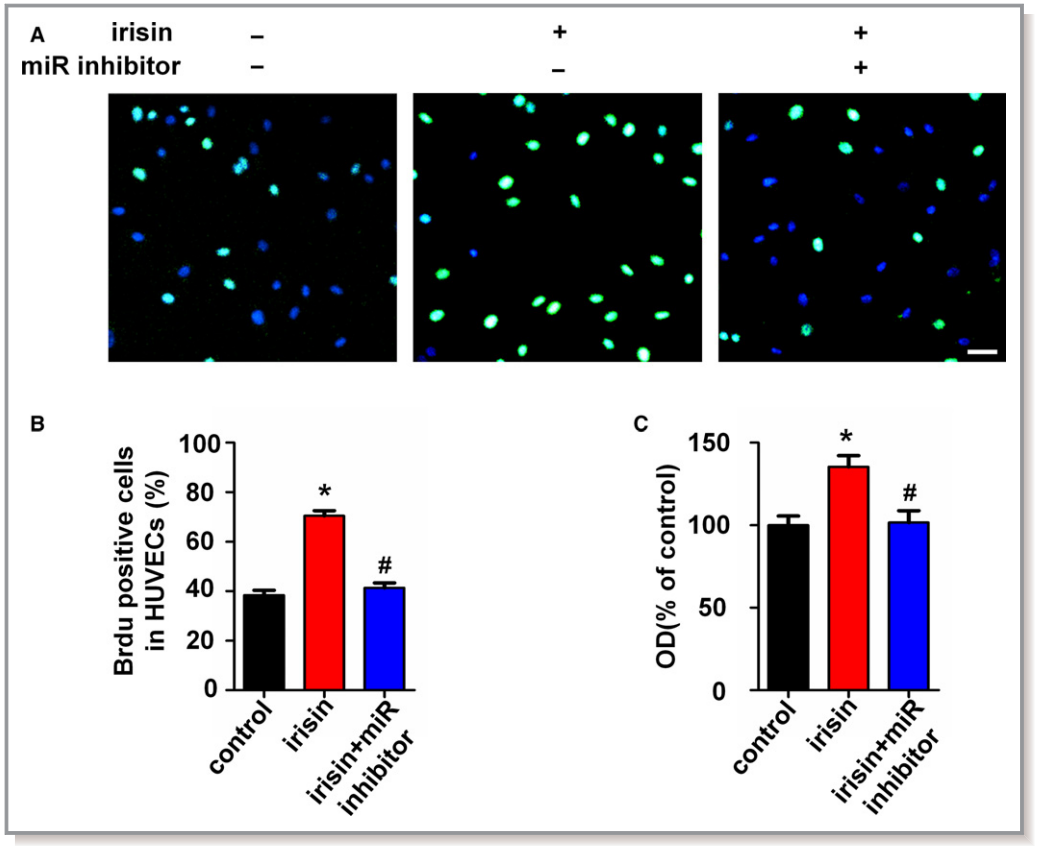

Figure 4. MicroRNA126-5p (miR126-5p) mediates the irisin-induced endothelial proliferation. Human umbilical vein endothelial cells (HUVECs) were transfected with the miR126-5p inhibitor or negative control for 6 hours followed by irisin treatment. (A) The HUVEC proliferation was measured using the BrdU incorporation assay. Scale bar indicates 80 μm. (B) Proliferation was assessed by the ratio of the average number of BrdU-positive cells to total cells in 10 random high-magnification fields. (C) The effect of the miR126-5p inhibitor on irisin-induced HUVEC viability was measured using the CCK8 assay. The data are expressed as the mean±SEM of three independent experiments. *P<0.05 vs control. #P<0.05 vs the irisin-treated group.

after treatment with irisin and was abolished by pretreatment with U0126 for 30 minutes. Correspondingly, irisin-induced miR126-5p expression was downregulated after pretreatment with U0126 for 30 minutes (Figure 5B). Furthermore, to test whether the ERK phosphorylation was induced by miR126-5p expression after irisin treatment, cells were transfected with the miR126-5p inhibitor. The results showed that the miR126-5p inhibitor did not affect irisin-induced ERK phosphorylation (Figure 5C). These data imply that irisin may induce miR126-5p through the ERK signaling pathway. In addition, it is demonstrated that irisin improved endothelial function by activating eNOS phosphorylation.[17] Therefore, we used the miR126-5p inhibitor to test whether miR126-5p mediates irisin-induced phosphorylation of eNOS. Incubation of the HUVECs with irisin enhanced eNOS phosphorylation, while the miR126-5p inhibitor did not affect this phenomenon (Figure 5D).

Dlk1 is the Target Gene of miR-126-5p in Irisin-Treated HUVECs

It has been reported that Dlk1, SDF-1α, MMP7, and ADAM9, which are associated with cell proliferation, are direct targets of miR126-5p.[25,30,31] To investigate the target genes of irisin-induced miR126-5p, we detected the change of mRNA levels of these genes. As demonstrated in Figure 6A, Dlk1 was significantly decreased after irisin treatment, whereas the others were unaffected. Furthermore, Western blot analysis was used to investigate the effect of irisin on Dlk1 protein expression. Dlk1 protein expression was significantly reduced in HUVECs treated with irisin for 24 hours. However, Dlk1 expression was restored by the miR126-5p inhibitor after the HUVECs were treated with irisin for 24 hours (Figure 6B). Next, we confirmed targeting of Dlk1 by miR-126-5p and studied the effect of Dlk1 on irisin-induced HUVEC proliferation. As shown in Figure 6C, cellular Dlk1 protein levels were

successfully repressed by Dlk1 siRNA. Similar to irisin, treatment of the cells with Dlk1 siRNA increased HUVEC viability compared with the control group. As expected, silencing of Dlk1 restored the inhibitory effect of the miR126-5p inhibitor on irisin-induced HUVEC proliferation (Figure 6D). Taken together, these results suggest that Dlk1 was involved in the irisin-induced pro-proliferation effect, which was controlled by miR126-5p.

Inhibition of miR126-5p Abrogates Irisin-Mediated Inhibition of Neointima Formation and Pro-Proliferation of ECs in apoE-Deficient Mice After Carotid Artery Partial Ligation

To determine the role of miR126-5p on the anti-atherosclerosis effect of irisin, a miR126-5p antagomir was used to block the miR126-5p expression in the partial ligated carotid artery mouse model. qRT-PCR showed the successful inhibition of miR126-5p by the miR126-5p antagomir as compared with the negative control (Figure S1B). Based on findings in the cell culture model, we measured the miR126-5p level in carotid arteries of apoE-deficient mice using qRT-PCR. Consistent with the results from the cell culture model, the miR126-5p level in carotid arteries of apoE-deficient mice after treatment with irisin for 4 weeks was 2.78-fold higher than in the control group. Treatment of mice with the miR126-5p antagomir caused reduction of the irisin-induced miR126-5p expression in the carotid artery (Figure 7A). The inhibitory effect of irisin on neointima formation was abrogated by miR126-5p antagomir treatment (Figure 7B through 7D). Similar results were observed using immunofluorescent staining, which demonstrated that blocking miR126-5p expression abrogated irisin-mediated EC proliferation. When miR126-5p expression was downregulated by the miR126-5p antagomir (2.55±0.60%), the proliferation of ECs decreased significantly in the partial ligated carotid artery, as compared with irisin treatment (8.40±1.55%) (Figure 8).

Furthermore, we have previously demonstrated that irisin inhibited EC apoptosis both in vitro and in vivo.[19,28] In addition to proliferation, miRNAs can also mediate apoptosis of ECs.[24] Therefore, the role of miR126-5p in the inhibitory effect of irisin on EC apoptosis was explored in this study. TUNEL staining showed that irisin treatment decreased the cell apoptotic rate on the luminal side of the atherosclerotic lesions. The miR126-5p antagomir abolished the inhibitory effect of irisin (Figure S2A). To confirm this effect, Annexin V/PI staining was used to measure ox-LDL–induced ECs dysfunction in vitro. Flow cytometry results demonstrated that the miR126-5p antagomir attenuated the inhibitory effect of irisin on 80 μg/mL ox-LDL–induced HUVEC apoptosis (Figure S2B and S2C). These results imply that miR126-5p may participate in the inhibitory effect of irisin on EC apoptosis.

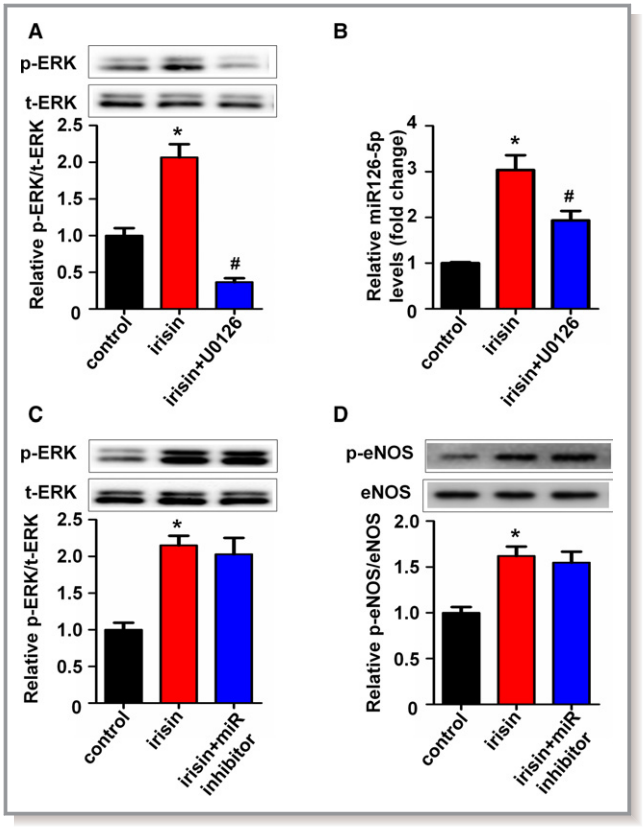

Figure 5. Irisin promotes ERK activation, which is required for microRNA126-5p (miR126-5p) expression. (A) Human umbilical vein endothelial cells (HUVECs) were pretreated with U0126 or untreated for 30 minutes and then incubated with irisin for 24 hours. ERK phosphorylation was determined by Western blot. Total ERK was used as a loading control. (B) Expression levels of miR126-5p in HUVECs after pretreatment with U0126 for 30 minutes were tested using quantitative real-time polymerase chain reaction. (C) HUVECs were transfected with the miR126-5p inhibitor or negative control for 6 hours followed by irisin treatment. ERK phosphorylation was determined by Western blot. Total ERK was used as a loading control. (D) eNOS phosphorylation was determined by Western blot. Total eNOS was used as a loading control. The data are expressed as the mean±SE of three independent experiments. **P*<0.05 vs control. #*P*<0.05 vs the irisin-treated group.

Effect of Irisin on Carotid Plaque Composition in Mice

Next, we analyzed the effect of irisin treatment on atherosclerotic composition and the role of miR126-5p by quantification of macrophage, lipid, and smooth muscle cell (SMC) content. As shown in Figure 9A and 9D, the CD68 positive macrophage area was reduced after irisin treatment. Interestingly, the miR126-5p antagomir abolished the inhibitory effect of

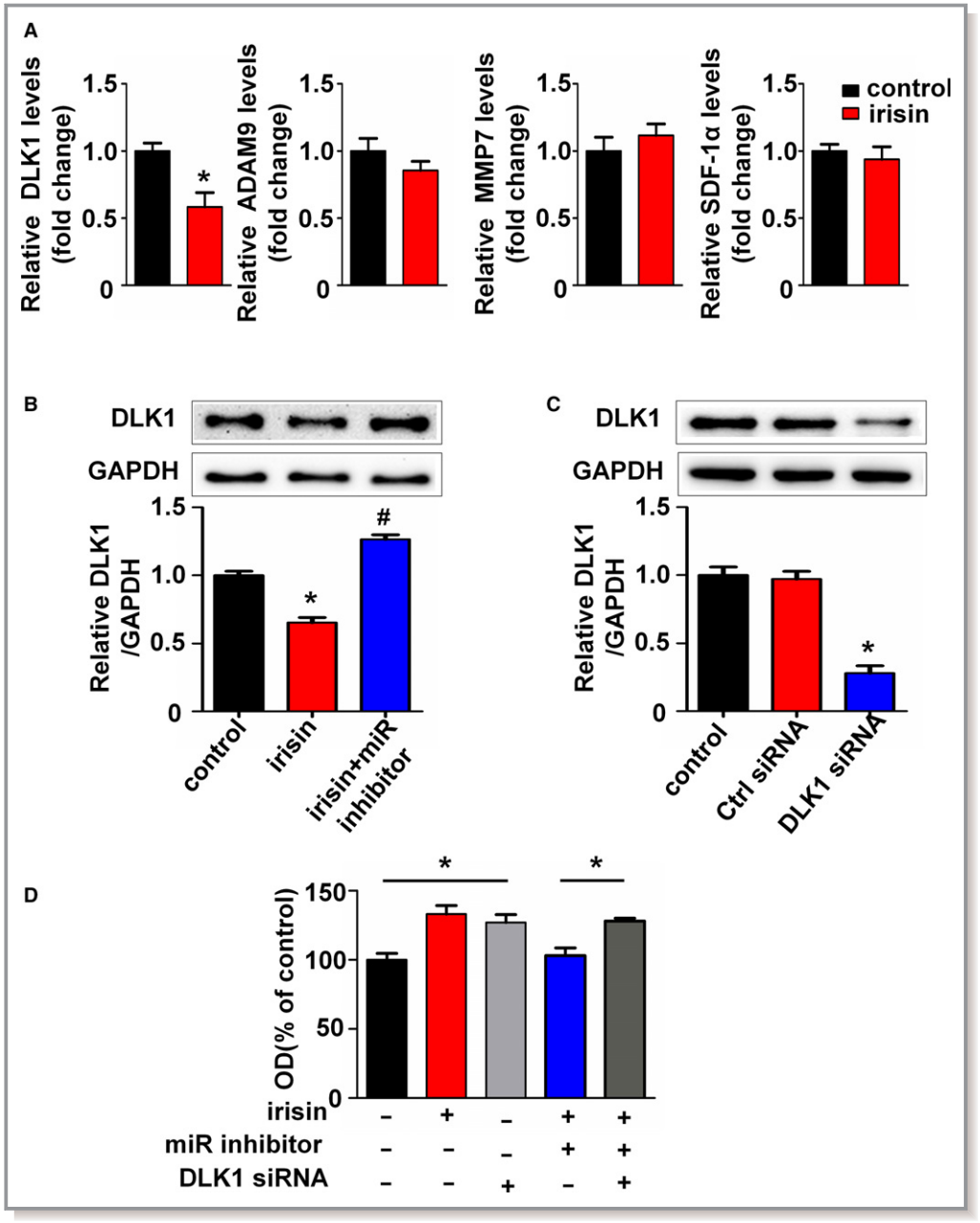

Figure 6. Dlk1 is the target gene of microRNA126-5p (miR126-5p) in irisin-treated human umbilical vein endothelial cells (HUVECs). (A) Expression levels of Dlk1, stromal-derived factor-1α (SDF-1α), MMP7, and ADAM9 mRNA in HUVECs were determined by real-time polymerase chain reaction and normalized to β-actin as indicated. (B) Western blotting analysis of Dlk1 expression levels in HUVECs. GAPDH was used as a loading control. (C) Western blots analysis of Dlk1 in HUVECs cotransfected with Dlk1 siRNA or negative control. (D) HUVECs were pretransfected with the miR126-5p inhibitor or Dlk1 siRNA before being treated with irisin, or left untreated. Vitality of HUVECs was measured using the CCK8 assay. The data are expressed as the mean±SE of three independent experiments. *P<0.05 vs control. $^{\#}P$<0.05 vs the irisin-treated group.

irisin on macrophage infiltration. Moreover, the lipid content tended to be decreased in irisin-treated mice, and the miR126-5p antagomir abolished this effect (Figure 9B and 9E). However, the lesional SMC area was not significantly different in all 3 groups (Figure 9C and 9F).

Discussion

The current study demonstrates that irisin can suppress neointima formation in the carotid partial ligation model of apoE-deficient mice by promoting EC proliferation.

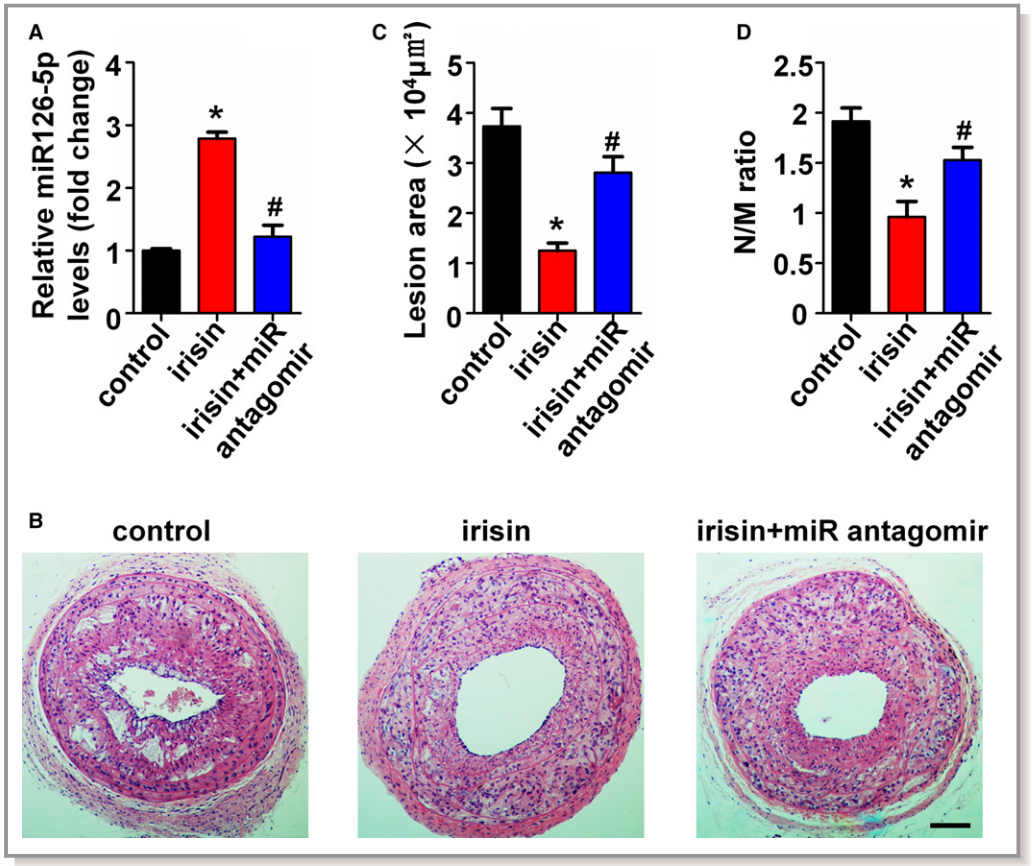

Figure 7. Inhibition of microRNA126-5p (miR126-5p) abolished irisin-mediated inhibition of neointima formation. The miR126-5p antagomir was applied to the adventitia around ligated artery segments during surgery (n=5). (A) miR126-5p expression in carotid arteries of apolipoprotein E (ApoE)–deficient mice were tested using quantitative polymerase chain reaction. (B) The effect of the miR126-5p antagomir on the irisin-induced inhibition of neointima formation was analyzed by hematoxylin-eosin staining. Scale bar indicates 100 μm. (C) Quantification of the neointima areas of the partially ligated carotid arteries is shown. (D) Degree of neointima formation 28 days after carotid ligation was calculated according to the neointima area to the media area (N/M) ratio. The data are expressed as mean±SE. **P*<0.05 vs control. #*P*<0.05 vs the irisin-treated group.

Furthermore, we have shown the involvement of miR126-5p in the pro-proliferation effect of irisin on HUVECs.

Various risk factors can induce EC injury and apoptosis, leading to endothelial dysfunction.[32,33] Endothelial dysfunction is the initial step in the development of atherosclerosis.[1,34,35] ECs with adequate survival and proliferation capacities are essential for the maintenance of endothelial integrity and repair of endothelial damage. Irisin, a newly discovered myokine, is released by skeletal muscle after exercise. Numerous scholars have conducted studies on the role of irisin and have demonstrated that irisin has potential therapeutic applications for metabolic disturbances.[11–13] Recently, many researchers have focused attention on the relationship between circulating irisin level and cardiovascular disease, such as vascular endothelial function.[14] Based on the results we previously demonstrated,[19,20] we presumed that irisin may have a protective effect on the development of atherosclerosis. In this study, we used the carotid partial ligation model, which has been extensively used in studies of vascular remodeling, to evaluate our hypothesis. The carotid partial ligation model was previously described as a model of disturbed blood flow that causes endothelial dysfunction and accelerated atherosclerosis.[36] Our findings show that irisin treatment for 4 weeks after carotid ligation decreased the severity of the neointima formation and rescued EC proliferation. This suggests that irisin improves vascular remodeling induced by carotid partial ligation, at least in part, by promoting the proliferation of vascular ECs.

Recently, miRNAs have been reported to be involved in EC functions. In the present study, using a miRNA array, we found that irisin treatment upregulated the expression of miR126-5p in HUVECs and miR126-5p may play a crucial role in irisin-induced EC proliferation. In the previous study, we have demonstrated that irisin can promote HUVEC proliferation by

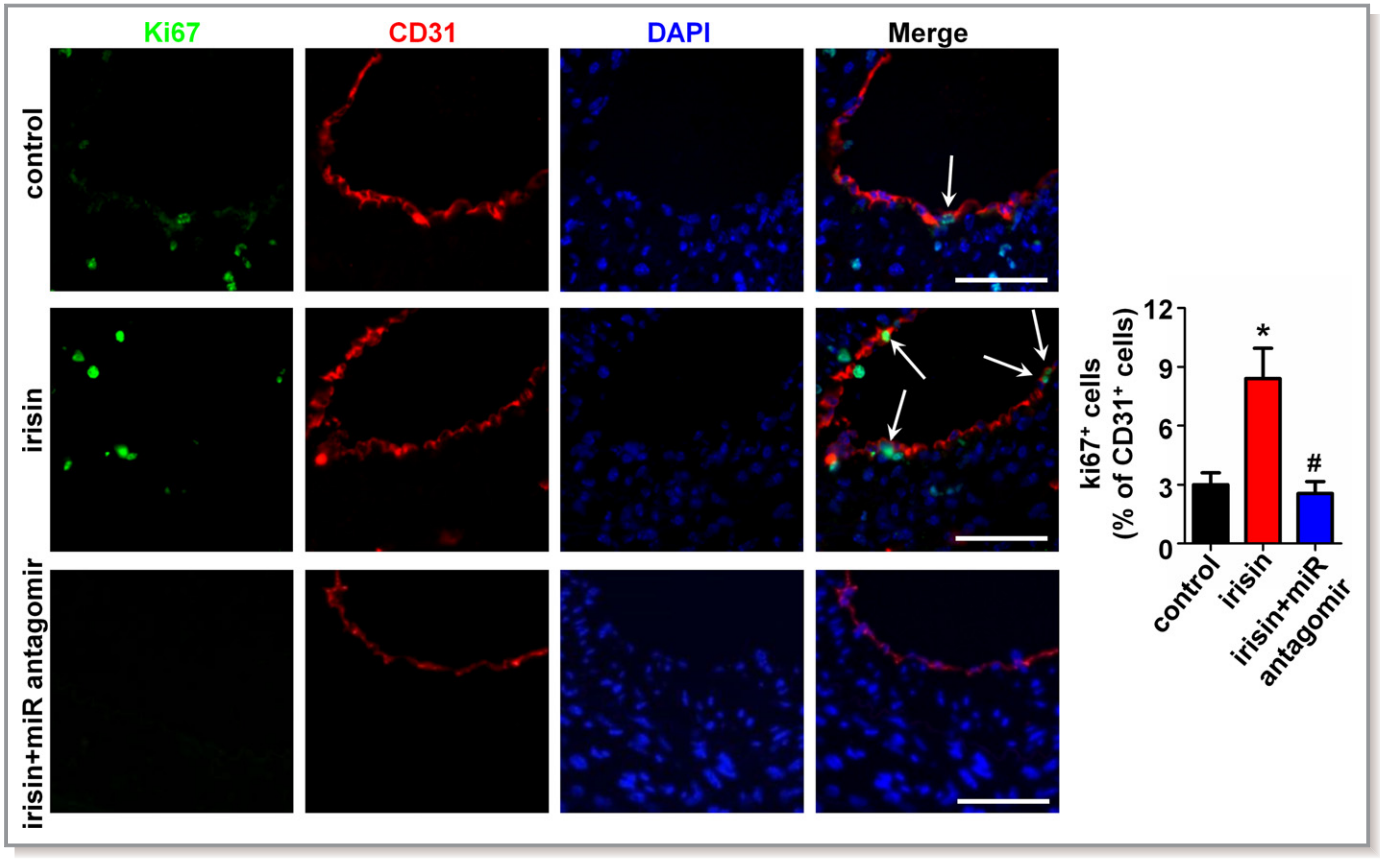

Figure 8. Inhibition of microRNA126-5p (miR126-5p) abolished irisin-mediated pro-proliferation of endothelial cells (ECs) in vivo. The effect of the miR126-5p antagomir on the irisin-induced EC proliferation was analyzed by double immunofluorescence staining for Ki67 and CD31. Representative images of Ki67 staining show proliferating cells (stained in green) in the endothelium. The nuclei were stained blue with 4′-6-diamidino-2-phenylindole (DAPI). CD31 (stained in red) was used as an endothelial marker. Arrows indicate $Ki67^{+}CD31^{+}$ cells. Scale bar indicates 50 μm. The data are expressed as mean±SE. $^{*}P<0.05$ vs control. $^{\#}P<0.05$ vs the irisin-treated group.

activating the ERK signaling pathway. Therefore, ERK inhibitor U0126 was used to clarify the relationship between ERK and miR126-5p. We showed that the induction of miR126-5p was associated with the activation of ERK signaling. Furthermore, our findings indicate that irisin may promote HUVEC proliferation through miR126-5p by suppressing Dlk1. Dlk1, also known as preadipocyte factor-1, inhibits angiogenesis by inhibiting EC proliferation, which has been attributed to its inhibitory effect on NOTCH1 activation.[37] Pretreatment with the miR126-5p inhibitor significantly attenuated endothelial protection by irisin and restored the protein levels of Dlk1. Those results are consistent with the previous report, which showed that Dlk1 is a direct target of miR-126-5p.[25] miR126-5p is processed from the precursor miRNA pre-miR-126, which is expressed in ECs and gives rise to two mature strands, the guide strand miR126-3p and the passenger strand miR126-5p. miR126-5p is expressed in various mouse and human tissues, and is among the most abundant miRNA in blood vessel ECs.[26,38] miR126-5p was reported to control EC activation and leucocyte trafficking.[38] In addition, we also explored the effect of irisin on EC apoptosis. The results imply that irisin can inhibit ligation-induced EC apoptosis in vivo and ox-LDL–induced HUVEC apoptosis in vitro through miR126-5p. Further studies are needed to confirm these findings and to better determine the underlying molecular mechanisms.

miRNAs are involved in a great variety of processes, which are linked to cardiovascular diseases[39] and atherosclerosis.[40] Our findings clearly indicate that the expression of miR126-5p was significantly increased in carotid arteries of apoE-deficient mice treated with irisin for 4 weeks. Moreover, miR126-5p inhibition abolished the inhibitory effects of irisin on neointima formation and the pro-proliferation effects on ECs in the carotid partial ligation mouse model. It suggests that the inhibitory effects of irisin on neointima formation by promoting EC proliferation may be through the upregulation of miR126-5p, which is in agreement with our in vitro data. Subsequently, we needed to explore the specific mechanisms for how reduced endothelial dysfunction reduces the intimal thickening induced by ligation. As expected, both lipid content and CD68-positive macrophage area are decreased in irisin-treated mice, and inhibiting miR126-5p abolished this inhibitory effect of irisin. Interestingly, the study by Zhang

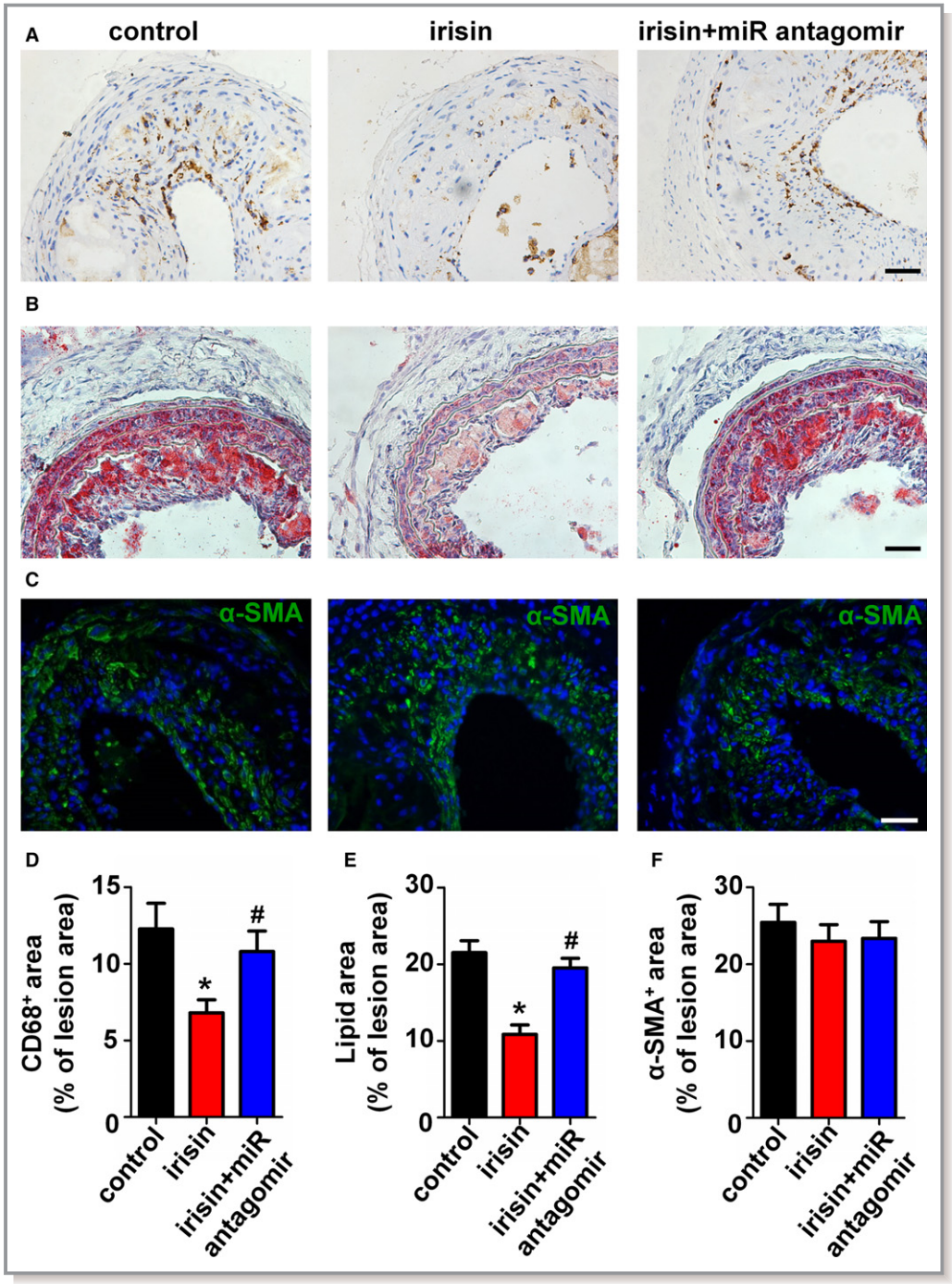

Figure 9. Irisin and the microRNA126-5p (miR126-5p) antagomir influenced plaque composition in vivo. (A) Representative pictures for CD68-positive plaque area and corresponding quantification. (B) Representative pictures for lipid content and corresponding quantification. (C) Representative pictures for α-smooth muscle actin (SMA)–positive (green) and nuclei (blue) plaque area and corresponding quantification. Scale bar indicates 50 μm. (D–F) Quantification of positive staining areas for Oil Red O (D), CD68 (E), and α-SMA (F). The data are expressed as mean±SE. **P*<0.05 vs control. #*P*<0.05 vs the irisin-treated group.

et al[30] has demonstrated that the ectopic expression of miR126-5p in breast tumor cells represses inflammatory monocyte recruitment into the tumor mass. However, neither irisin nor the miR126-5p antagomir was associated with the SMC content. Thus, our data suggest that irisin may reduce ligation-induced intimal thickening through protection of

endothelial dysfunction and also by inhibiting the recruitment of monocytes and the deposition of lipid.

Conclusions

We reported that irisin is an anti-atherogenic myokine, which specifically promotes EC proliferation by upregulating miR126-5p. This finding indicates that irisin treatment could serve as a potential therapeutic strategy to protect against atherosclerosis development.

Sources of Funding

This work was supported by the Taishan Scholar Fund, the National Natural Science Foundation of China (81570407), the Traditional Chinese Medicine Technology Development Program in Shandong Province (2013-183), and the Major State Basic Research Development Program of China (973 Program) (2015CB553600).

Disclosures

None.

References

1. Lusis AJ. Atherosclerosis. *Nature*. 2000;407:233–241.
2. Peters SA, den Ruijter HM, Bots ML, Moons KG. Improvements in risk stratification for the occurrence of cardiovascular disease by imaging subclinical atherosclerosis: a systematic review. *Heart*. 2012;98:177–184.
3. Peng N, Meng N, Wang S, Zhao F, Zhao J, Su L, Zhang S, Zhang Y, Zhao B, Miao J. An activator of mTOR inhibits oxLDL-induced autophagy and apoptosis in vascular endothelial cells and restricts atherosclerosis in apolipoprotein E(-)/(-) mice. *Sci Rep*. 2014;4:5519.
4. Triggle CR, Samuel SM, Ravishankar S, Marei I, Arunachalam G, Ding H. The endothelium: influencing vascular smooth muscle in many ways. *Can J Physiol Pharmacol*. 2012;90:713–738.
5. Libby P. Inflammation in atherosclerosis. *Nature*. 2002;420:868–874.
6. Itoh Y, Toriumi H, Yamada S, Hoshino H, Suzuki N. Resident endothelial cells surrounding damaged arterial endothelium reendothelialize the lesion. *Arterioscler Thromb Vasc Biol*. 2010;30:1725–1732.
7. Yong Qiao X, Nie Y, Xian Ma Y, Chen Y, Cheng R, Yao Yinrg W, Hu Y, Ming Xu W, Zhi Xu L. Irisin promotes osteoblast proliferation and differentiation via activating the MAP kinase signaling pathways. *Sci Rep*. 2016;6:18732.
8. Bostrom P, Wu J, Jedrychowski MP, Korde A, Ye L, Lo JC, Rasbach KA, Bostrom EA, Choi JH, Long JZ, Kajimura S, Zingaretti MC, Vind BF, Tu H, Cinti S, Hojlund K, Gygi SP, Spiegelman BM. A PGC1-alpha-dependent myokine that drives brown-fat-like development of white fat and thermogenesis. *Nature*. 2012;481:463–468.
9. Zhang Y, Li R, Meng Y, Li S, Donelan W, Zhao Y, Qi L, Zhang M, Wang X, Cui T, Yang LJ, Tang D. Irisin stimulates browning of white adipocytes through mitogen-activated protein kinase p38 MAP kinase and ERK MAP kinase signaling. *Diabetes*. 2014;63:514–525.
10. Jedrychowski MP, Wrann CD, Paulo JA, Gerber KK, Szpyt J, Robinson MM, Nair KS, Gygi SP, Spiegelman BM. Detection and quantitation of circulating human irisin by tandem mass spectrometry. *Cell Metab*. 2015;22:734–740.
11. Stengel A, Hofmann T, Goebel-Stengel M, Elbelt U, Kobelt P, Klapp BF. Circulating levels of irisin in patients with anorexia nervosa and different stages of obesity–correlation with body mass index. *Peptides*. 2013;39:125–130.
12. Liu JJ, Wong MD, Toy WC, Tan CS, Liu S, Ng XW, Tavintharan S, Sum CF, Lim SC. Lower circulating irisin is associated with type 2 diabetes mellitus. *J Diabetes Complications*. 2013;27:365–369.
13. Park KH, Zaichenko L, Brinkoetter M, Thakkar B, Sahin-Efe A, Joung KE, Tsoukas MA, Geladari EV, Huh JY, Dincer F, Davis CR, Crowell JA, Mantzoros CS. Circulating irisin in relation to insulin resistance and the metabolic syndrome. *J Clin Endocrinol Metab*. 2013;98:4899–4907.
14. Xiang L, Xiang G, Yue L, Zhang J, Zhao L. Circulating irisin levels are positively associated with endothelium-dependent vasodilation in newly diagnosed type 2 diabetic patients without clinical angiopathy. *Atherosclerosis*. 2014;235:328–333.
15. Hou N, Han F, Sun X. The relationship between circulating irisin levels and endothelial function in lean and obese subjects. *Clin Endocrinol*. 2015;83:339–343.
16. Zhu D, Wang H, Zhang J, Zhang X, Xin C, Zhang F, Lee Y, Zhang L, Lian K, Yan W, Ma X, Liu Y, Tao L. Irisin improves endothelial function in type 2 diabetes through reducing oxidative/nitrative stresses. *J Mol Cell Cardiol*. 2015;87:138–147.
17. Han F, Zhang S, Hou N, Wang D, Sun X. Irisin improves endothelial function in obese mice through the AMPK-eNOS pathway. *Am J Physiol Heart Circ Physiol*. 2015;309:H1501–H1508.
18. Jiang M, Wan F, Wang F, Wu Q. Irisin relaxes mouse mesenteric arteries through endothelium-dependent and endothelium-independent mechanisms. *Biochem Biophys Res Commun*. 2015;468:832–836.
19. Song H, Wu F, Zhang Y, Zhang Y, Wang F, Jiang M, Wang Z, Zhang M, Li S, Yang L, Wang XL, Cui T, Tang D. Irisin promotes human umbilical vein endothelial cell proliferation through the ERK signaling pathway and partly suppresses high glucose-induced apoptosis. *PLoS One*. 2014;9:e110273.
20. Wu F, Song H, Zhang Y, Zhang Y, Mu Q, Jiang M, Wang F, Zhang W, Li L, Li H, Wang Y, Zhang M, Li S, Yang L, Meng Y, Tang D. Irisin induces angiogenesis in human umbilical vein endothelial cells in vitro and in zebrafish embryos in vivo via activation of the ERK signaling pathway. *PLoS One*. 2015;10:e0134662.
21. Bartel DP. MicroRNAs: genomics, biogenesis, mechanism, and function. *Cell*. 2004;116:281–297.
22. Stellos K, Dimmeler S. Vascular microRNAs: from disease mechanisms to therapeutic targets. *Circ Res*. 2014;114:3–4.
23. Neth P, Nazari-Jahantigh M, Schober A, Weber C. MicroRNAs in flow-dependent vascular remodelling. *Cardiovasc Res*. 2013;99:294–303.
24. Tang Y, Zhang YC, Chen Y, Xiang Y, Shen CX, Li YG. The role of miR-19b in the inhibition of endothelial cell apoptosis and its relationship with coronary artery disease. *Sci Rep*. 2015;5:15132.
25. Schober A, Nazari-Jahantigh M, Wei Y, Bidzhekov K, Gremse F, Grommes J, Megens RT, Heyll K, Noels H, Hristov M, Wang S, Kiessling F, Olson EN, Weber C. MicroRNA-126-5p promotes endothelial proliferation and limits atherosclerosis by suppressing Dlk1. *Nat Med*. 2014;20:368–376.
26. Fish JE, Santoro MM, Morton SU, Yu S, Yeh RF, Wythe JD, Ivey KN, Bruneau BG, Stainier DY, Srivastava D. miR-126 regulates angiogenic signaling and vascular integrity. *Dev Cell*. 2008;15:272–284.
27. Menghini R, Casagrande V, Cardellini M, Martelli E, Terrinoni A, Amati F, Vasa-Nicotera M, Ippoliti A, Novelli G, Melino G, Lauro R, Federici M. MicroRNA 217 modulates endothelial cell senescence via silent information regulator 1. *Circulation*. 2009;120:1524–1532.
28. Zhang Y, Mu Q, Zhou Z, Song H, Zhang Y, Wu F, Jiang M, Wang F, Zhang W, Li L, Shao L, Wang X, Li S, Yang L, Wu Q, Zhang M, Tang D. Protective effect of irisin on atherosclerosis via suppressing oxidized low density lipoprotein induced vascular inflammation and endothelial dysfunction. *PLoS One*. 2016;11:e0158038.
29. Sullivan CJ. Flow-dependent remodeling in the carotid artery of fibroblast growth factor-2 knockout mice. *Arterioscler Thromb Vasc Biol*. 2002;22:1100–1105.
30. Zhang Y, Yang P, Sun T, Li D, Xu X, Rui Y, Li C, Chong M, Ibrahim T, Mercatali L, Amadori D, Lu X, Xie D, Li QJ, Wang XF. miR-126 and miR-126* repress recruitment of mesenchymal stem cells and inflammatory monocytes to inhibit breast cancer metastasis. *Nat Cell Biol*. 2013;15:284–294.
31. Felli N, Felicetti F, Lustri AM, Errico MC, Bottero L, Cannistraci A, De Feo A, Petrini M, Pedini F, Biffoni M, Alvino E, Negrini M, Ferracin M, Mattia G, Care A. miR-126&126* restored expressions play a tumor suppressor role by directly regulating ADAM9 and MMP7 in melanoma. *PLoS One*. 2013;8:e56824.
32. Pober JS, Min W, Bradley JR. Mechanisms of endothelial dysfunction, injury, and death. *Annu Rev Pathol*. 2009;4:71–95.
33. Deanfield JE, Halcox JP, Rabelink TJ. Endothelial function and dysfunction: testing and clinical relevance. *Circulation*. 2007;115:1285–1295.
34. Dimmeler S, Hermann C, Zeiher AM. Apoptosis of endothelial cells. Contribution to the pathophysiology of atherosclerosis? *Eur Cytokine Netw*. 1998;9:697–698.
35. Sun X, Belkin N, Feinberg MW. Endothelial microRNAs and atherosclerosis. *Curr Atheroscler Rep*. 2013;15:372.

36. Nam D, Ni CW, Rezvan A, Suo J, Budzyn K, Llanos A, Harrison D, Giddens D, Jo H. Partial carotid ligation is a model of acutely induced disturbed flow, leading to rapid endothelial dysfunction and atherosclerosis. *Am J Physiol Heart Circ Physiol*. 2009;297:H1535–H1543.

37. Rodriguez P, Higueras MA, Gonzalez-Rajal A, Alfranca A, Fierro-Fernandez M, Garcia-Fernandez RA, Ruiz-Hidalgo MJ, Monsalve M, Rodriguez-Pascual F, Redondo JM, de la Pompa JL, Laborda J, Lamas S. The non-canonical NOTCH ligand DLK1 exhibits a novel vascular role as a strong inhibitor of angiogenesis. *Cardiovasc Res*. 2012;93:232–241.

38. Poissonnier L, Villain G, Soncin F, Mattot V. miR126-5p repression of ALCAM and SetD5 in endothelial cells regulates leucocyte adhesion and transmigration. *Cardiovasc Res*. 2014;102:436–447.

39. Small EM, Olson EN. Pervasive roles of microRNAs in cardiovascular biology. *Nature*. 2011;469:336–342.

40. Hulsmans M, De Keyzer D, Holvoet P. MicroRNAs regulating oxidative stress and inflammation in relation to obesity and atherosclerosis. *FASEB J*. 2011;25:2515–2527.

SUPPLEMENTAL MATERIAL

Figure S1.

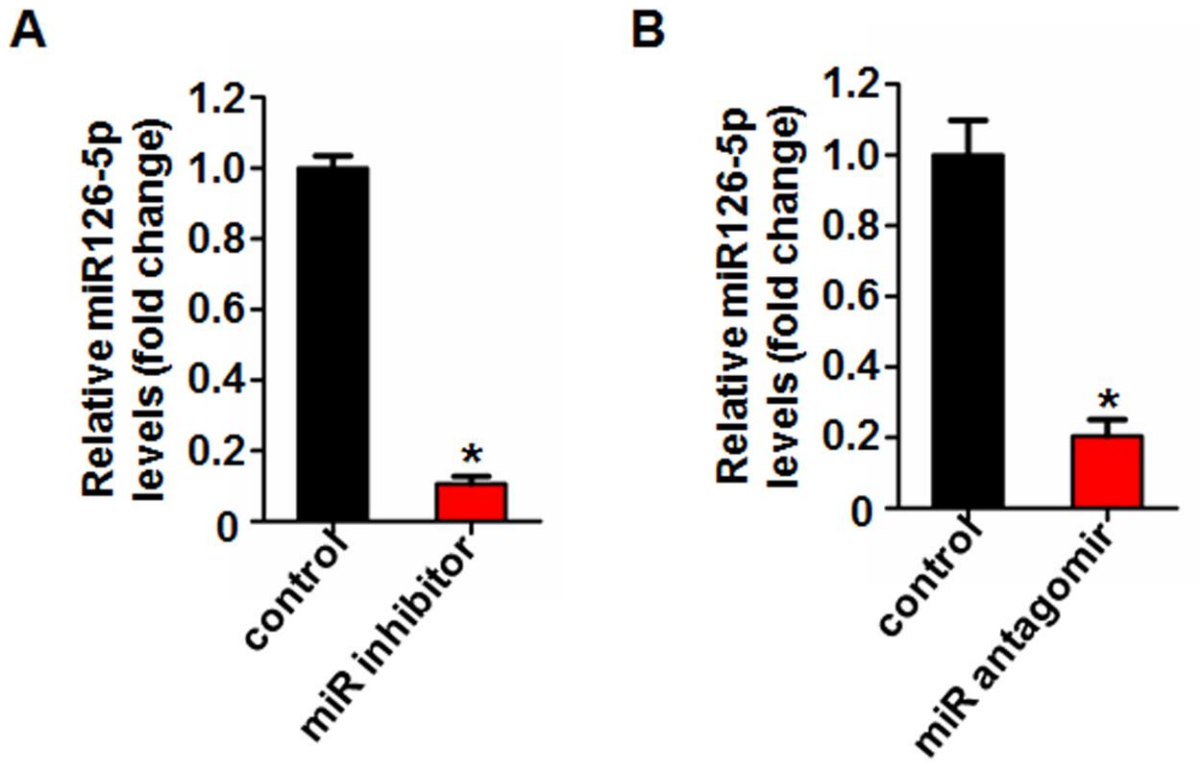

Figure S1. miR126-5p levels after transfection of the miR126-5p inhibitor in vitro and the miR126-5p antagomir in vivo. (*A*) HUVECs were transfected as indicated. At 24 h post transfection, cellular RNAs were isolated for detection of miR126-5p using qRT-PCR. (*B*) The miR126-5p antagomir was applied to the partial ligated carotid artery for 4 weeks, and RNAs were isolated for detection of miR126-5p using qRT-PCR. The data were normalized to that of negative control samples. The data were expressed as the mean ± SEM of three independent experiments. *P < 0.05 vs. control.

Figure S2.

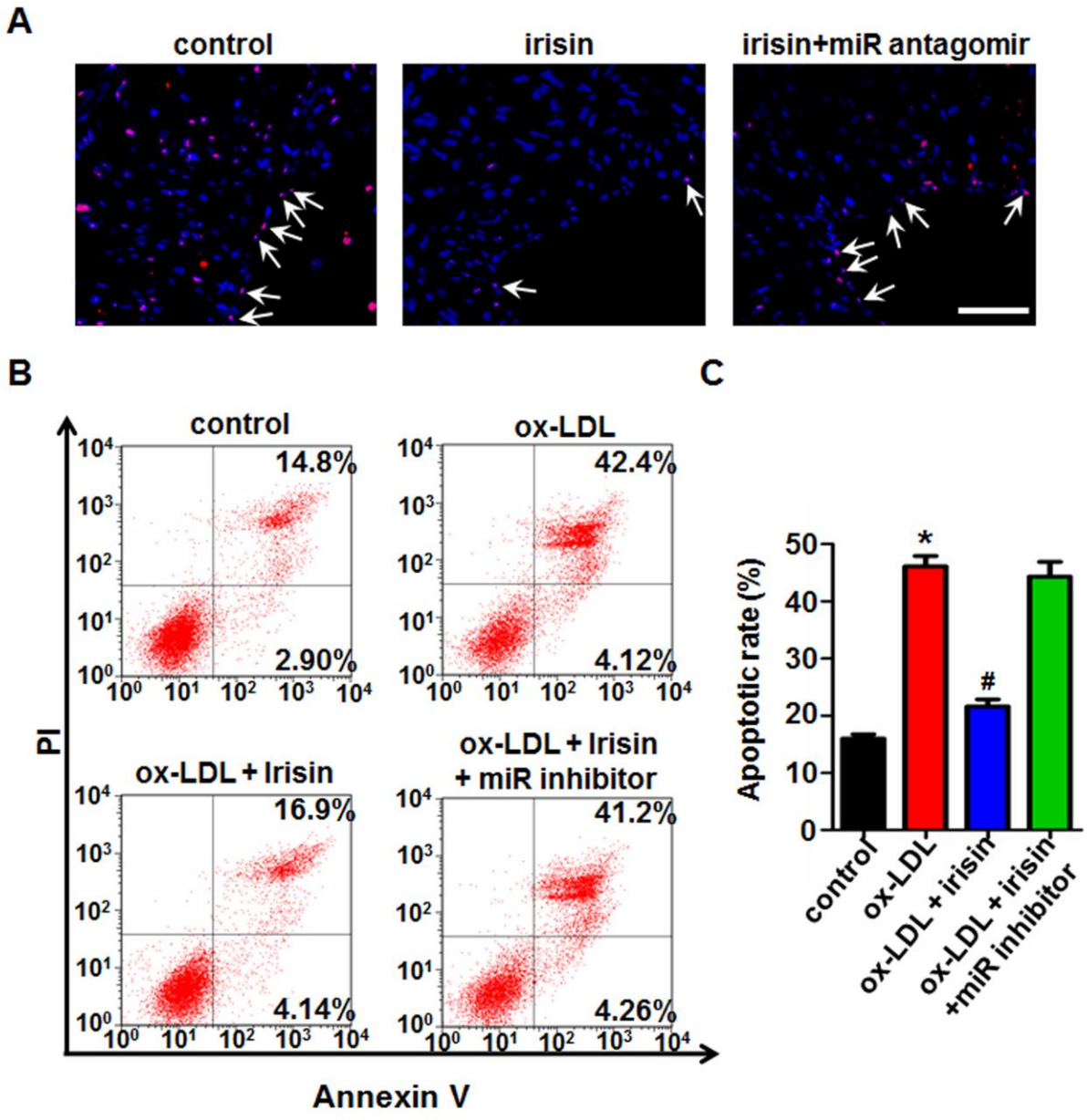

Figure S2. miR126-5p mediated the inhibitory effect of irisin on ox-LDL induced EC apoptosis. (*A*) Sections from the mice carotid arteries were labeled by TUNEL to detect apoptotic cells and counterstained with DAPI to detect nuclei. Scale bar

indicates 50 μm. (*B*) HUVECs were transfected with the miR126-5p inhibitor or negative control for 6h followed by irisin and/or ox-LDL treatment. Apoptosis of HUVECs was detected by using flow cytometry. (*C*) The apoptotic rate was determined by calculating the ratio of Annexin-V-positive and Annexin-V/PI-double positive cells to total cells. The data were expressed as the mean ± SEM of three independent experiments. *P < 0.05 vs. control, # P < 0.05 vs. ox-LDL -treated group.